Available online at www.sciencedirect.com
ScienceDirect
Journal of Molecular Graphics and Modelling 25 (2007) 616–632
Journal of Molecular Graphics and Modelling
www.elsevier.com/locate/JMGM

Molecular modeling of hexakis(areneisonitrile)technetium(I), tricarbonyl η^5 cyclopentadienyl technetium and technetium(V)-oxo complexes: MM3 parameter development and prediction of biological properties

Peter Wolohan, David E. Reichert *

Mallinckrodt Institute of Radiology, Washington University School of Medicine, St. Louis, MO 63110, United States

Received 1 December 2005; received in revised form 26 April 2006; accepted 27 April 2006
Available online 16 May 2006

Abstract

Genetic algorithms (GA) were used to develop specific technetium metal–ligand force field parameters for the MM3 force field. These parameters were developed using automated procedures within the program FFGenerAtor from a combination of crystallographic structures and *ab initio* calculations. These new parameters produced results in good agreement with experiment when tested against a blind validation set. To illustrate the utility of these new force field parameters, quantitative structure–activity relationship (QSAR) models were developed to predict the P-glycoprotein uptake ($\log_{10}$ VI) of a series of hexakis(areneisonitrile)technetium(I) complexes and to predict their biodistribution. The $\log_{10}$ VI QSAR model, built using a training set of 16 Tc(I) isonitrile complexes, exhibited a correlation between the experimental $\log_{10}$ VI and 5 simple descriptors as follows: $r^2 = 0.94$, $q^2 = 0.93$. When applied to an external test set of six Tc(I) isonitrile complexes, the QSAR preformed with great accuracy $q^2 = 0.78$ based on a leave-one-out cross-validation analysis. Further QSAR models were developed to predict the biodistribution of the same set of Tc(I) isonitrile complexes; a QSAR model to predict hepatic uptake exhibited a correlation between the experimental $\log_{10}$(Blood/Liver) with six simple descriptors as follows: $r^2 = 0.97$, $q^2 = 0.96$. A QSAR model to predict renal uptake exhibited a correlation between the experimental $\log_{10}$(Blood/Kidney) and six simple descriptors as follows: $r^2 = 0.85$, $q^2 = 0.82$. When applied to the external test set the QSAR models preformed with great accuracy, $q^2 = 0.78$ and 0.56, respectively.
© 2006 Elsevier Inc. All rights reserved.

Keywords: Technetium; MM3 parameters; QSAR; P-glycoprotein

1. Introduction

The radionuclide ^{99m}Tc is the most widely utilized radionuclide for diagnostic imaging in nuclear medicine. This is a result of several factors, its high specific activity and availability though the ^{99}Mo generator, its convenient 6 h half-life, and its emission of a 140 keV γ-ray with 89% abundance which is ideal for imaging with the standard gamma cameras found in almost all hospitals. The Federal Drug Administration (FDA) has approved numerous technetium radiopharmaceuticals for use as diagnostic imaging agents [1–3].

^{99m}Tc-sestamibi (Fig. 1) is approved for myocardial perfusion imaging and breast cancer [4], and it is also used for the functional detection *in vivo* of human multidrug resistance (MDR1) P-glycoprotein (Pgp) expression in human tissue [5,6]. [^{99m}Tc] TRODAT-1 (Fig. 1) based on a diaminodithiol radionuclide chelate and a tropane precursor is a primary ligand used to image the dopamine transporter [7]. The dopamine transporter (DAT), which is found in the presynaptic neurons concentrated in the striatum of the brain, has been found to play an important role in Parkinson's disease, addiction and schizophrenia [8]. Tc(I)-tetrakis(*tert*-butylisonitrile) radiometal complexes containing a bidentate aromatic dye moiety such as Congo Red have been used to image Alzheimer's disease as a result of their binding to β1–40 amyloid fibrils [9].

The diaminodithiol Tc(V)-oxo scaffold together with tricarbonyl technetium steroid based derivatives (Fig. 1) have been used to develop imaging agents for the nuclear hormone

* Corresponding author at: Mallinckrodt Institute of Radiology, Washington University School of Medicine, 510 S. Kingshighway Campus Box 8225, St. Louis, MO 63110, United States. Tel.: +1 314 362 8461; fax: +1 314 362 9940.
E-mail address: reichertd@wustl.edu (D.E. Reichert).

1093-3263/$ – see front matter © 2006 Elsevier Inc. All rights reserved.
doi:10.1016/j.jmgm.2006.04.007

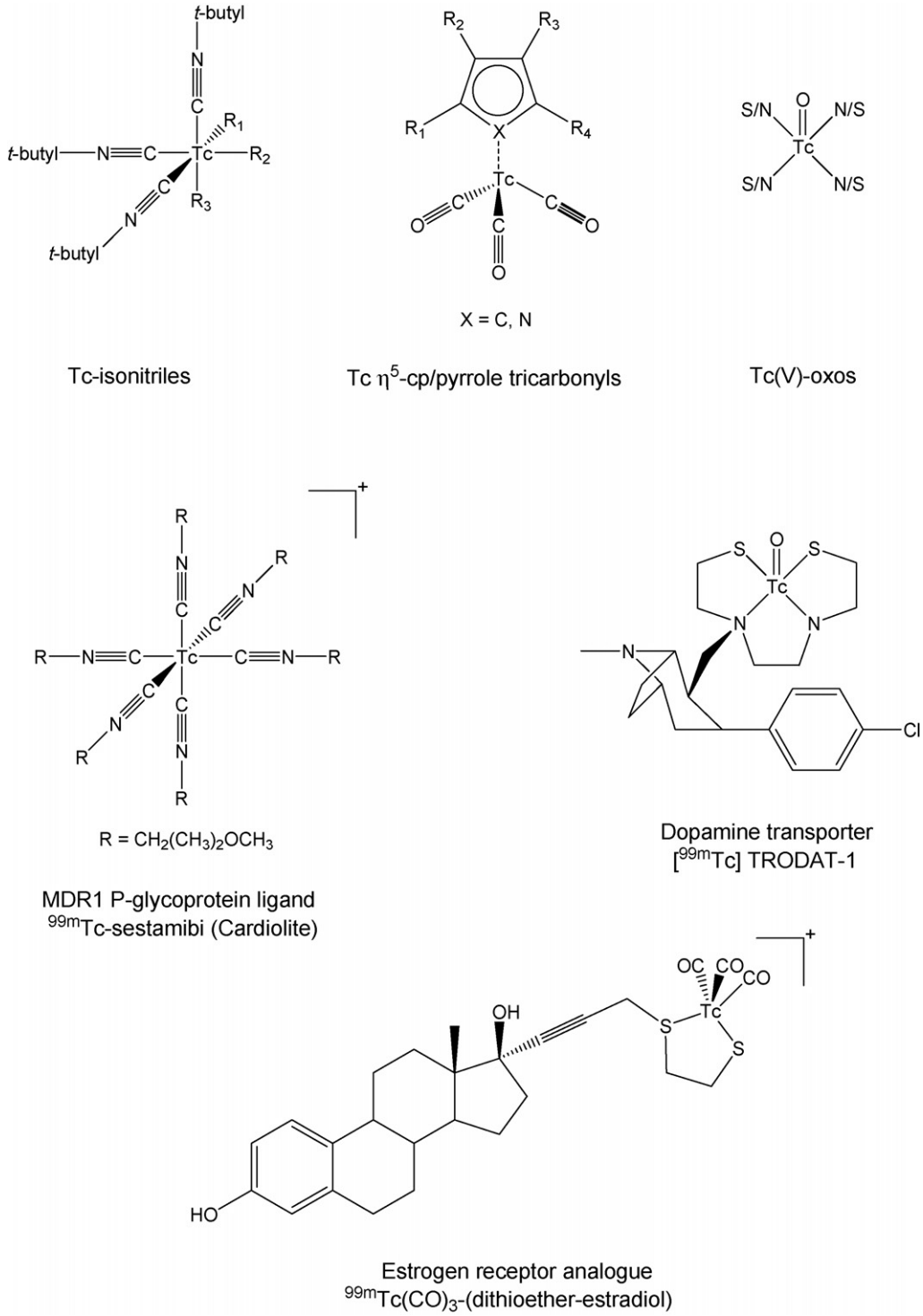

Fig. 1. Classes of technetium chelates studied and several important technetium radiopharmaceuticals.

steroid receptors [10–13]. These receptors are implicated in the function of various cancers including breast cancer and prostate cancer. Finally, bifunctional chelates (BFCs) where the technetium radionuclide chelate is coupled to a biological targeting molecule such as a monoclonal antibody or a peptide have also been developed [2]. Considering the amount of time, effort, and cost in bringing new imaging agents to the clinic, the ability to understand and predict the bioavailability and activity of technetium radiometal complexes is a priority in order to aid the development of novel technetium based imaging agents. There can be little doubt that the development of tools or models to streamline this process would be of worth to the community.

Quantitative structure–activity relationships (QSAR) have become a common tool in the field of molecular modeling since their introduction [14]. Indeed, they have found application in

both the prediction of biological activity and more recently in the prediction of the absorption, distribution, metabolism, excretion and toxicological (ADME/tox) properties of organic drug-like compounds [15–19]. While QSAR methods have found many applications in the modeling of the properties of organic drug-like compounds they have found little application with radiometal complexes until our recent work, possibly due to the lack of the required metal–ligand parameters [20]. With the development of suitable metal–ligand force field parameters, the adoption of QSAR studies will no doubt aid the search for novel metal-based pharmaceuticals targeted towards biological receptors.

The MM3 force field developed by Allinger et al. [21] is one of the most accurate force fields available for the modeling of organic ligands [22]. Several researchers have successfully developed specific metal–ligand parameters compatible with this accurate force field [23,24]. The MM3 force field describes the energy of a molecule with a simple algebraic expression consisting of terms describing bond stretching, angle bending, dihedral rotation and intermolecular forces, such as electrostatics, van der Waals interactions and hydrogen bonding. The constants in these equations are obtained from experimental data or *ab initio* calculations.

The development of specific metal–ligand force field parameters consists of determining these constants within the framework of the algebraic expression of the force field being used and is commonly achieved via two main methods. The first method utilizes a traditional optimization algorithm such as the Newton–Raphson or Simplex techniques while the second, and probably most promising method, utilizes a genetic algorithm (GA) [24–26]. Both methods approach this multi-dimensional problem from the same starting point in that they attempt to find a common set of parameters which reproduce most accurately the crystallographic X-ray structure of a training set of metal complexes. We have adopted the GA approach of Strassner et al. [24] within the framework of their automated parameter program FFGenerAtor in this work.

2. Experimental

Technetium ligand complexes were modeled using the MM3 force field as implemented in the molecular modeling package TINKER [27] running on an SGI workstation. The implementation of the MM3 force field in TINKER is the full Allinger MM3(1999) force field including parameters for pi-systems. In the TINKER MM3 implementation, the directional hydrogen bonding term is included, but the negligible anomeric and Bohlmann correction terms are not implemented. X-ray structures representative of three classes of important technetium radiopharmaceuticals (Fig. 1) were taken from the Cambridge Structural Database [28] (CSD) and manipulated with the program MOLDEN [29], which provides a convenient interface between the CSD and TINKER.

The reference data for the technetium parameters involved a total of 14 technetium containing crystal structures, shown in Figs. 2 and 3. The first set of eight technetium containing crystal structures were predominately tricarbonyl technetium complexes (refcodes: DUCRAU, ZUDHIP, GIZGUR, KITDAS, NUMRES, KITDIA, WIJPAG, ZETNAN) while the second six were predominately technetium(V)-oxo complexes (refcodes: CITLAS, GIKZEF, JOTZAT, SUKROF, TOXMEY, WACRUN).

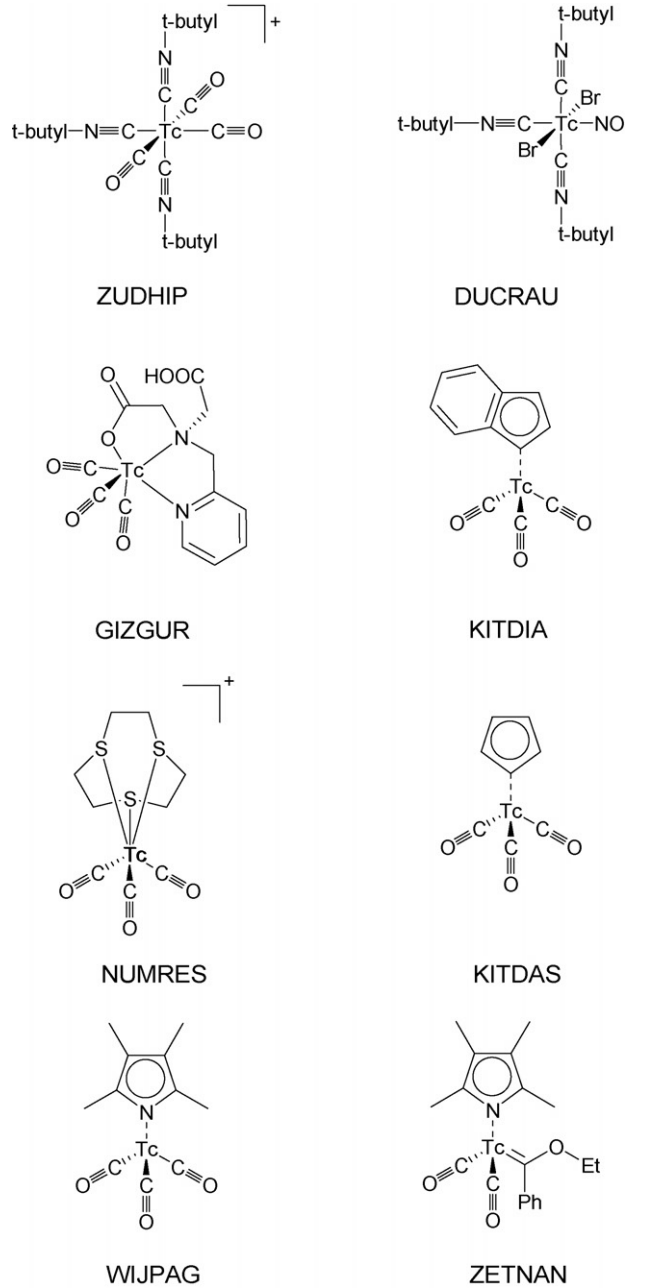

Fig. 2. Reference compounds used to develop the Tc(I)-isonitrile and Tc(0)-η^5 cyclopentadienyl tricarbonyl parameters.

From MOLDEN, a TINKER input file was generated for each of the technetium complexes. At this point, a series of new MM3 force field atom types were defined allowing for the development of force field parameters not present in the MM3 force field. These new force field parameters included the definition of new MM3 parameters for a six- and eight-coordinate technetium atom, eight-coordinate representing the η^5 coordination of a five-membered ring, together with definitions for coordinating organic ligands. For example,

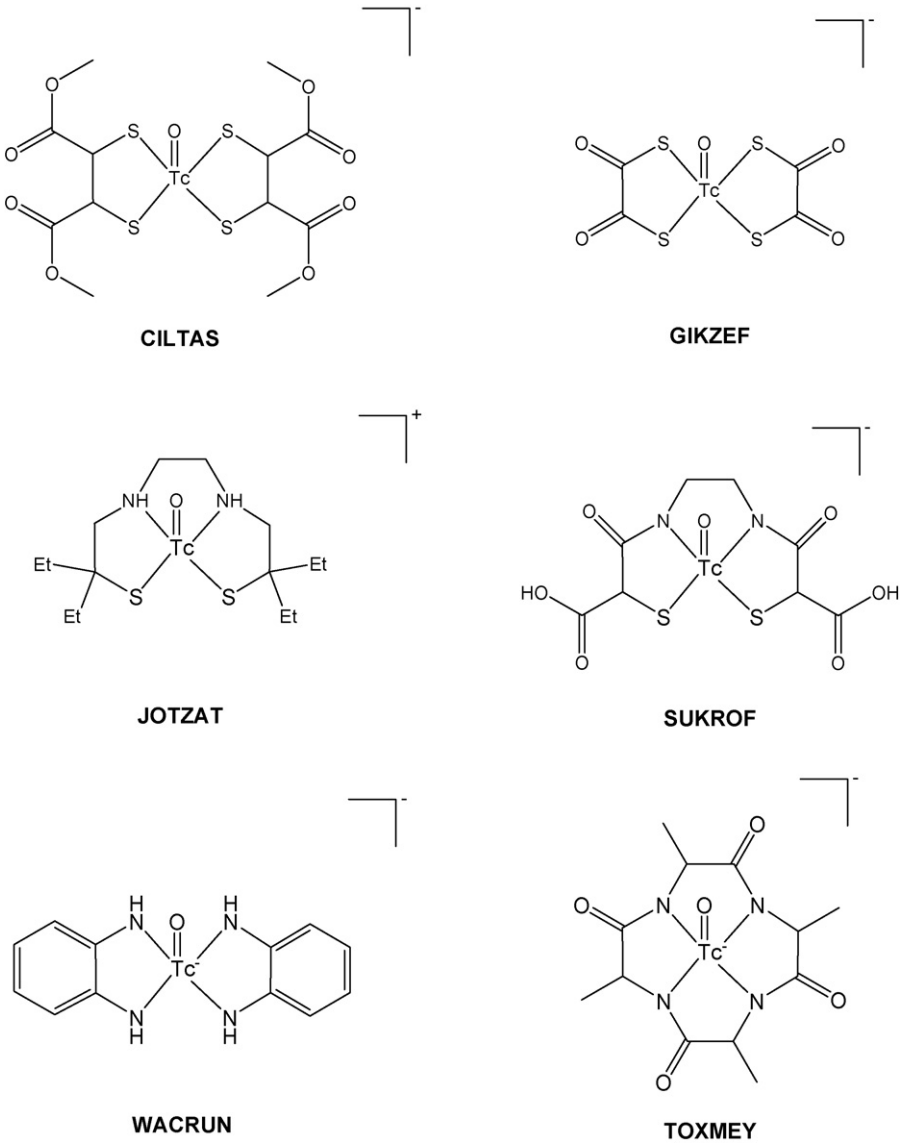

Fig. 3. Reference compounds used to develop the Tc(V) oxo parameters.

looking at tricarbonyl-(η^5-pentamethyl-cyclopentadienyl)-technetium [KITDAS] an eight-coordinate Tc atom type was defined, together with a new cyclopentadienyl carbon C*sp*^{2}, a new carbonyl C*sp* atom type and finally a new carbonyl O*sp* atom type.

These force field parameters were optimized using the automated parameter development program FFGenerAtor which utilizes a GA. Following the work of Strassner et al. [24], a steady state GA using a roulette selector together with a crossover rate of 0.9 and a mutation rate of 0.1 was used for each run. Within the GA, the force field parameters were represented by chromosomes of real numbers. Within a population, each individual chromosome is constructed of genes that correspond to the missing parameters, i.e. bond, angle, torsion and out of plane bending parameters. Initial values for these parameters were taken from an average of the corresponding experimental value following structural analysis of the reference structures from the CSD. Bond lengths were allowed to optimize within a range of ±0.5 Å of this average while angles were allowed to optimize within a range of ±30°. Associated force constants were constrained to a range of 0–250 mdyn/Å and 0–40 mdyn/rad^2, respectively. Coding of the torsional parameters is more arbitrary because of the shear number of these missing parameters hence the need to impose flexible boundaries for these terms in order to allow the GA to optimize fully. As a result, torsional angles were allowed to optimize within a range of −180° to 180° and their associated constants were constrained to a range of ±200 kcal/mol. Only force field bond lengths, angles and dihedrals involving the newly defined atom types were optimized, the original MM3 parameters were not altered.

Initial guesses for the coded parameters from the GA were fed into the force field making it now possible to minimize each starting X-ray structure using TINKER's optimize program. Once minimized TINKER's superpose routine was used to calculate the root-mean-squared deviation (rmsd), most

commonly in massweighted coordinates, between the two structures. The rmsd was then used to generate a fitness value for each newly developed parameter set which in turn guides the GA. The cycle is repeated for a number of GA cycles which we set to 750 generations. Electrostatic point charges were added to the final force field parameters following the procedure of Bayly et al., using the programs RESP and Jaguar5.0 [30,31]. The input for RESP is the electrostatic potential calculated from a full quantum mechanical optimization of a crystal structure. Crystal structures representative of each of the new force field atom types had their geometries optimized at the density functional level of theory (B3LYP/LACVP*+) using Jaguar.

The end result is a set of newly defined force field parameters whose fitness to both the reference set of structures and a blind validation set of structures can be evaluated based on the average rmsd, the goal being to produce a set of robust parameters which accurately reproduce the X-ray structure of a diverse set of related structures, an average rmsd below 0.400 being indicative of accuracy.

2.1. Parameter testing

Seven crystal structures were chosen as a validation set of the tricarbonyl technetium parameters (Fig. 4): VIVLER, MUXZAG, TAYPOY, WACXIH, KITDEW and AMUCAM, an analogue of the important radiopharmaceutical ^{99m}Tc-sestamibi (Cardiolite). These independent structures were minimized with the developed parameter set and compared to the X-ray crystal structure as an accuracy test. In the same way, six structures were chosen as a validation set of the Tc(V)-oxo parameters (Fig. 5): BATMTC, JIDLOX, LIGKUH, VUDVAR, VUDVEV and WAVGEF. In addition, several of the complexes in this validation set resemble the building blocks of

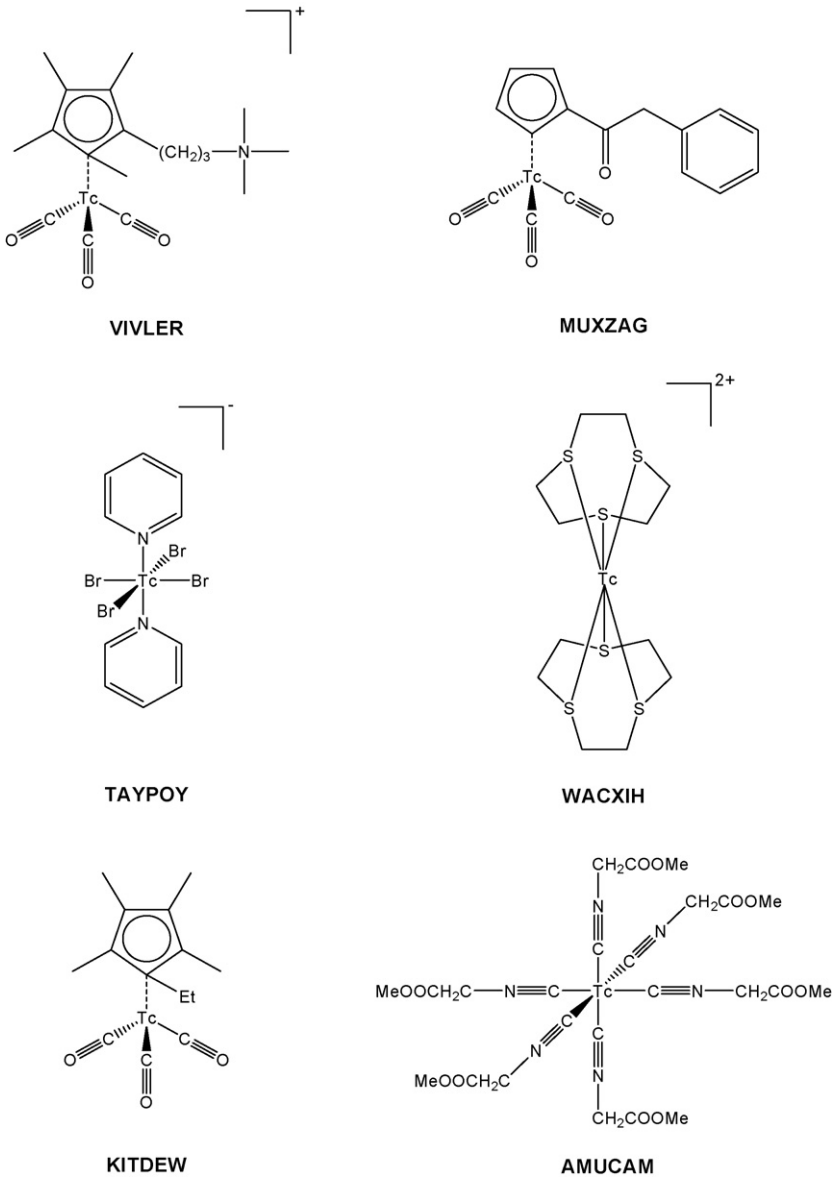

Fig. 4. Validation complexes used to test the Tc(I)-isonitrile and Tc(0)-η^5 cyclopentadienyl tricarbonyl parameters.

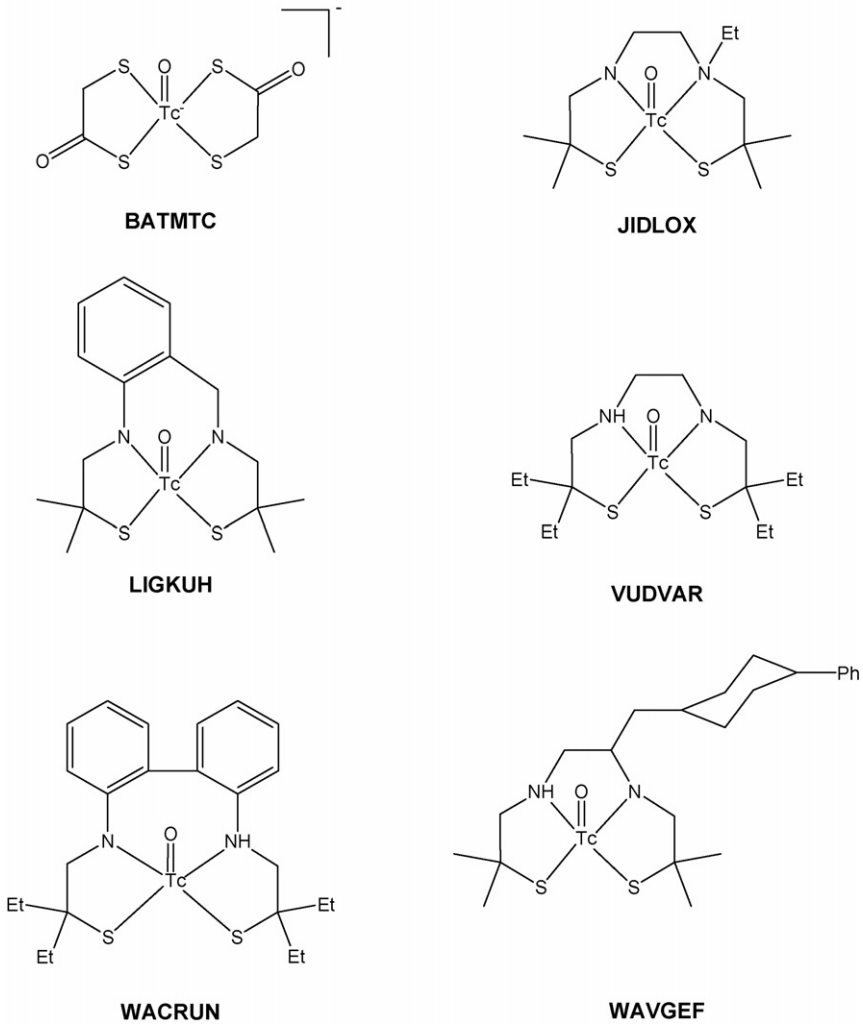

Fig. 5. Validation complexes used to test the Tc(V) oxo parameters.

the diaminodithiol technetium based radiopharmaceuticals (Fig. 1). It is important to note that the structures in the validation sets serve as an independent test of the parameters as they were not utilized in developing the parameters.

At this point, the newly developed MM3 technetium force field parameters from both the predominately tricarbonyl technetium complexes and technetium(V)-oxo complexes were combined to form a complete MM3 force field parameter file. Exhaustive testing was carried out by reproducing the rmsd for all structures in the reference datasets with the combined parameters to ensure no conflicts.

2.2. QSAR modeling

For the QSAR modeling, a total of 21 hexakis(areneisonitrile)technetium(I) complexes and ^{99m}Tc-sestamibi with their experimental data were taken from Herman et al. [32], were built and their structures optimized with the developed MM3 parameters. The experimental data consisted of the verapamil index (VI) and biodistribution data for each of the complexes. The verapamil index represents the ratio of net uptake of the technetium complex in multidrug resistance (MDR) Pgp cells in the presence of verapamil, the classical MDR Pgp modulator, over control. In essence, technetium complexes transported by Pgp in the cells would exhibit a $VI > 1$ because of low accumulation in the control and verapamil-induced accumulation. Those binding competitively would exhibit a $VI < 1$ because of verapamil-induced displacement. The biodistribution data consisted of hepatic and renal uptake based on the %ID/g (the percentage of the injected radioactivity found in an organ, normalized by the weight of that organ), the ratio of Blood/Liver represents hepatic accumulation while Blood/Kidney represents renal uptake.

Since the experimental structure of none of the 21 hexakis(areneisonitrile)technetium(I) complexes or ^{99m}Tc-sestamibi were available a related analogue was used as a template. The most appropriate template being the X-ray structure of AMUCAM used in the tricarbonyl technetium validation set was utilized as the template for constructing models. These structures were then minimized using the developed MM3 force field parameters and TINKER's optimize program. Extensive sampling of the conformational space of both the arene moiety and the functional groups of all of the technetium complexes were performed using TINKER's

scan program. Once a viable model of each of the 22 structures was obtained the structures were transferred to the program MOE [33] for QSAR modeling. Once in MOE the atomic partial charges for each structure were replaced with atomic charges calculated using the partial equalization of orbital electronegativities (PEOE) method of Gasteiger and Marsili, in order to provide a more consistent description of electrostatics [34]. Two-dimensional schematics of all the structures are included in Tables 4 and 5.

Within the program MOE, 170 molecular descriptors were calculated for each of the 22 structures. These molecular descriptors attempt to describe basic concepts such as shape, size, internal charge distribution and lipophilicity through a myriad of terms which when combined can be used to construct a quantitative relationship to an experimental property such as biological activity [19]. For the $\log_{10}$ VI QSAR, a test set of six structures was selected at random from the complete set of 22 compounds leaving a training set of 16 structures. The number of molecular descriptors used in the model was drastically reduced by evaluating their individual statistical significance to the experiment data, a process commonly referred to as pruning the descriptors. Similarly, QSAR models were constructed to model the experimental biodistribution data.

In QSAR equations, n is the number of observations, r^2 the correlation coefficient utilizing a partial least squares (PLS) analysis, q^2 the cross-validated correlation coefficient utilizing a leave-one-out analysis, RMSE the root mean square error, SEE_{cv} the associated cross-validated root mean square error and F is a measure of the statistical significance of the correlation. While q^2 is the traditional measure of the quality of the fit a value above 0.50 suggesting a predictive model.

3. Results and discussion

While technetium has several oxidations state available, we have focused our modeling efforts on the two most prevalent in clinically used compounds Tc(I) and Tc(V). An additional constraint on our structure choices was the availability of a relatively large dataset of biological data allowing QSARs to be developed. In this work, we sought to model the P-glycoprotein uptake ($\log_{10}$ VI) and biodistribution of a series of hexakis(areneisonitrile)technetium(I) complexes hence an emphasis on the known isonitrile structures DUCRAU and ZUDHIP. Given that few Tc isonitrile structures exist in the CSD the Tc(I) dataset was supplemented by a series of cyclopentadienyl tricarbonyl technetium(I) structures. As shown by Alberto and others, the tridentate Cp ligand offers several advantages for utilization in radiopharmaceuticals, such as small volume and low molecular weight [35].

In more than 90% of the known mono-oxo Tc(V) structures, the coordination sites are occupied by N, O or S [36]. Neutral or negatively charged Tc(V)-oxo tetradentate complexes have served as the basic scaffolding for the vast majority of technetium based imaging agents. One of the most commonly utilized ligand types are the N_2S_2 chelates containing ionizable thiol groups. For our parameter development, we focused on parameters capable of modeling these commonly utilized structures.

In order to accurately model the structure of these classes of technetium complexes, we developed a set of technetium ligand specific parameters for the MM3 force field using the genetic algorithm approach of Strassner et al. [24]. The massweighted root-mean-squared deviation (rmsd) of each of the structures in the predominately tricarbonyl technetium reference and validation sets are shown in Table 1. As can be seen in Table 1, the GA developed MM3 parameters were able to reproduce the X-ray structures with good accuracy; the reference set exhibited an average rmsd of 0.293. A similar level of accuracy was maintained (rmsd = 0.312) when the parameters were used to reproduce the X-ray structures of the seven compounds in the blind validation set (Fig. 4). Upon further analysis, it is apparent that the accuracy of the reference set was adversely affected by the force field parameters inability to accurately model the structures of the two isonitrile technetium(I) analogues DUCRAU and ZUDHIP. This is most likely due to the large degree of conformational freedom present in the coordinating groups, making it difficult to develop a unique set of force field parameters which describe them with great accuracy. Indeed, this is further illustrated by the worse performance of the developed parameters in describing the structure of AMUCAM. It is clear that an improved force field could be developed based on a larger

Table 1
Comparison of calculated MM3 structure to X-ray for Tc(I)-isonitriles and Tc-tricarbonyl η^5 cyclopentadienyl reference set and validation set

Reference set		Validation set	
Refcode	rmsd (Å) MM3 (GA)	Refcode	rmsd (Å) MM3 (GA)
DUCRAU	0.467	VIVLER	0.260
ZUDHIP	0.526	MUXZAG	0.189
GIZGUR	0.376	TAYPOY	0.059
KITDAS	0.080	WACXIH	0.205
NUMRES	0.221	KITDEW	0.404
KITDIA	0.126	AMUCAM	0.757
WIJPAG	0.131		
ZETNAN	0.414		
Average	0.293		0.312

Table 2
Comparison of calculated MM3 structure to X-ray for Tc(V)-oxo reference set and validation set

Reference set		Validation set	
Refcode	rmsd (Å) MM3 (GA)	Refcode	rmsd (Å) MM3 (GA)
CILTAS	0.205	BATMTC	0.182
GIKZEF	0.102	JIDLOX	0.118
JOTZAT	0.127	LIGKUH	0.087
SUKROF	0.381	VUDVAR	0.395
TOXMEY	0.087	VUDVEV	0.515
WACRUN	0.070	WAVGEF	0.527
Average	0.162		0.304

Table 3
Bond stretching MM3 parameters for Tc(I) and Tc(V) oxo's

MM3 atom type and force field identifier	Bond stretching parameter	
	Bond length (Å)	Force constant (mdyn/Å)
Tc(I)		
Tc(215)–$C_{carbonyl}$(222)	1.81	7.50
Tc(215)–$C_{cyclopentadienyl}$(221)	2.22	7.59
Tc(215)–$N_{aromatic}$(219)	2.17	4.80
Tc(215)–C_{sp^2}(2)	1.96	9.08
Tc(214)–$C_{carbonyl}$(222)	1.97	4.17
Tc(214)–$C_{nitrile}$(216)	2.09	4.17
Tc(214)–Br(224)	2.51	1.33
Tc(214)–$N_{nitrosyl}$(225)	1.65	7.72
Tc(214)–S(218)	1.32	2.00
Tc(214)–$N_{aromatic}$(219)	2.06	6.78
Tc(214)–N_{amine}(220)	2.35	7.93
Tc(214)–$O_{carboxyl}$(75)	2.11	5.01
Tc(V)		
Tc(226)=O(227)	1.65	2.12
Tc(226)–S(228)	2.30	5.21
Tc(226)–N_{sp^2}(229)	1.93	3.37
Tc(226)–N_{sp^3}(230)	2.10	4.00

The numbers in parentheses indicate the MM3 atom types involved in the bond.

dataset of isonitrile technetium(I) analogues if that experimental information were available. However, the developed parameters do an adequate job and the technetium isonitrile core is reproduced with excellent accuracy.

Having successfully developed parameters for the tricarbonyl and isonitrile technetium complexes we moved on to developing parameters for the technetium(V)-oxo complexes. The results from the MM3 parameter development for the six X-ray structures (Fig. 3) are shown in Table 2. Although a smaller dataset, hence requiring a smaller number of interdependent parameters to be developed, the average rmsd of both the reference set and the blind validation set (Fig. 5) of structures exhibit excellent accuracy 0.162 and 0.304, respectively. Table 3 illustrates the new bond stretching parameters developed in this study; the entire parameter set is available in supplementary data.

In addition to an analysis of the rmsd's, our force field was able to reproduce several key features with good accuracy. For example, the elongated Tc-Nsp^3 bond length of 2.22 Å in JIDLOX is 2.11 Å in our minimized structure while a similar elongated Tc-Nsp^3 in GIZGUR of 2.32 Å is well modeled at 2.37 Å in our minimized structure. The ability to reproduce these elongated metal–ligand bonds is further evidence of a robust force field.

3.1. QSAR modeling of MDR Pgp cell uptake and biodistribution

In order to illustrate the utility of the development of new metal–ligand force field parameters, we endeavoured to use our new MM3 parameters to build QSAR models of experimental biological data. The biological data chosen consisted of $\log_{10}$ VI and the biodistributions of 21 hexakis(areneisonitrile)technetium(I) complexes as well as ^{99m}Tc-sestamibi from animal models. The competitive uptake of any targeted radiopharmaceutical in the specific protein receptor of interest is of course critical. For example, if a developed radiopharmaceutical does not show sufficient *in vivo* affinity for its targeted receptor the ability to image the function and expression of that receptor target is greatly diminished [12]. While cellular uptake can give an indication of how a radiopharmaceutical binds to a target, *in vivo* biodistribution studies in animals, most commonly rodents, describe the whole body distribution, clearance pathways, and metabolism of a compound at different time-points.

Table 4
Results from QSAR model of the verapamil index ($\log_{10}$ VI) of Tc(I)-isonitrile complexes

QSAR	r^2	q^2	RMSE	$RMSE_{cv}$	n_{mols}	$n_{descriptors}$
$\log_{10}$ VI model (training set)	0.94	0.93	0.09	0.09	16	5
$\log_{10}$ VI model (test set)	0.10	0.78	0.26	0.50	6	5

$\log_{10} VI_{exp}$ refers to the $\log_{10}$ of the experimental verapamil index, the verapamil index represents the ratio of net uptake in the presence of verapamil over control, r^2 to the non-validated correlation, q^2 to the cross-validated correlation, RMSE to the root mean square error and $RMSE_{cv}$ refers to the cross-validated root mean square error.

The results from the $\log_{10}$ VI QSAR analysis for both the training set of 16 technetium radiopharmaceuticals and the test set of six technetium radiopharmaceuticals are shown in Table 4. Here, a predictive QSAR model was developed utilizing only five descriptors exhibiting a cross-validated correlation coefficient, q^2, of 0.93 and small cross-validated error, $RMSE_{cv}$, exceeding the 0.50 benchmark for q^2. This conclusion is supported by the performance of the same QSAR in predicting the $\log_{10}$ VI's of the six compounds in the blind test set. Here, the corresponding $q^2 = 0.78$ which is also well above the benchmark 0.50. The associated chemical structures together with the $\log_{10}$ VI QSAR calculated, experimental and corresponding residual difference for both the training set (Table 5) and test set (Table 6) are shown. The corresponding QSAR equation is given below:

$$\begin{aligned}\log_{10} VI_{calc} = {} & 2.165 + (0.001 \times \text{PEOE_VSA-1}) \\ & - (0.01 \times \text{PEOE_VSA-6}) \\ & + (2.00 \times \text{PEOE_VSA_FPPQS}) \\ & + (0.020 \times \text{a_count}) - (0.072 \times \text{a_nC}) \qquad (1)\end{aligned}$$

Three of the predictive descriptors (PEOE) are based on the partial charge analysis of Gasteiger and Marsili [34] The VSA extension refers to the fitting of the calculated partial charges to the van der Waals surface of the molecule while the further extensions, i.e. +0, −0 and refer to a summation of the surface area where the partial charge falls between 0.00 and 0.05 for the

Table 5
Comparison of calculated and experimental verapamil index ($\log_{10}$ VI) of Tc(I)-isonitrile complexes in QSAR training set

	Structure	$\log_{10}$ VI_{exp}	$\log_{10}$ VI_{calc}	Δ
MIBI	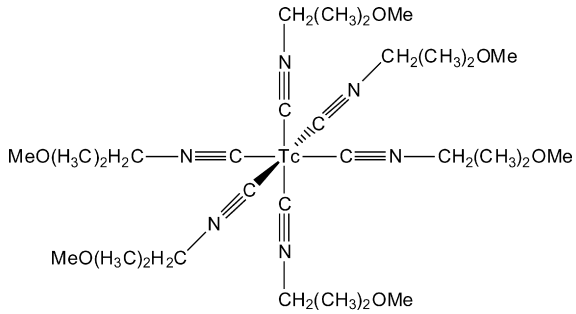	1.52	1.52	0.00
1a	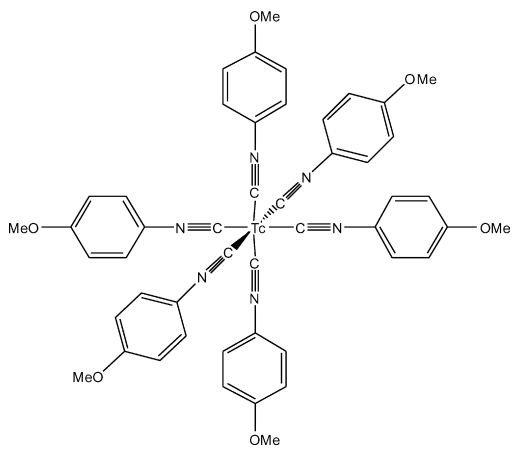	0.37	0.41	0.04
1c	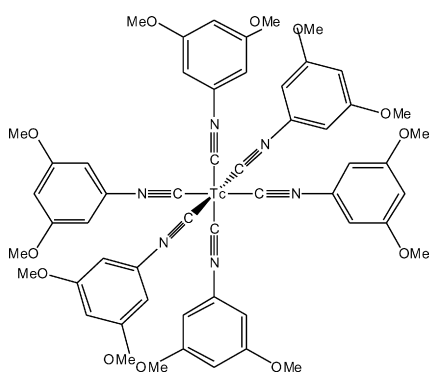	0.26	0.35	0.09
1d	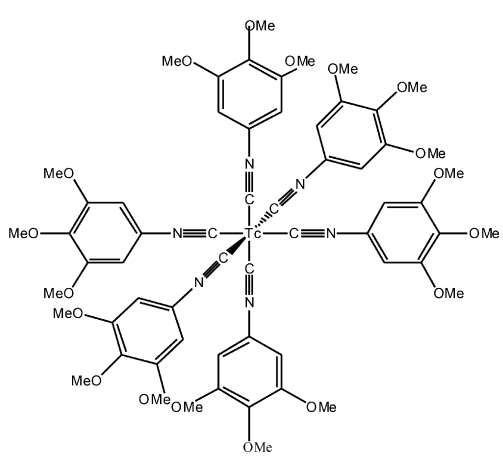	0.47	0.29	−0.18

Table 5 (*Continued*)

	Structure	$\log_{10}$ VI$_{exp}$	$\log_{10}$ VI$_{calc}$	Δ
1f	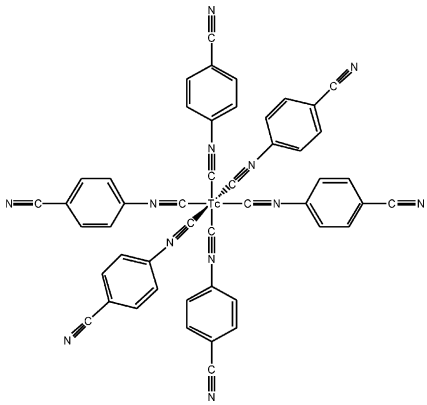	0.21	0.17	−0.04
1g	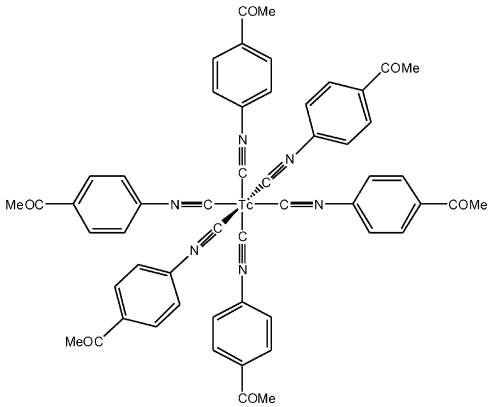	0.24	0.22	−0.02
1i	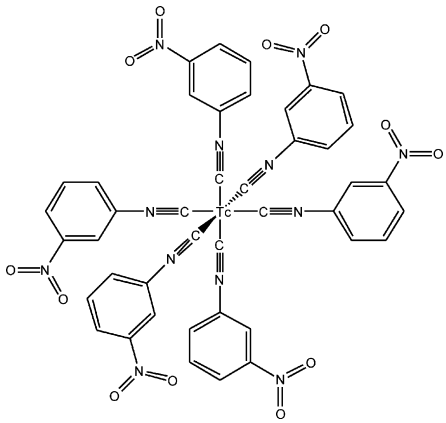	<−0.01	0.07	0.07
1j	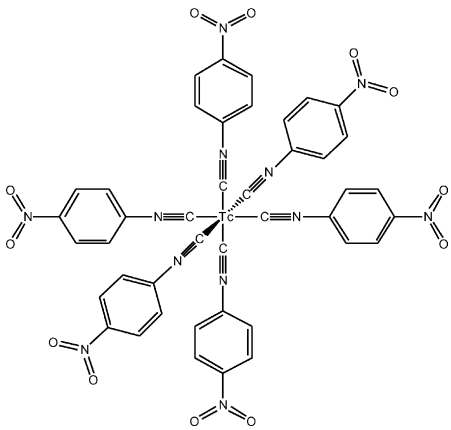	0.06	0.04	−0.02

Table 5 (*Continued*)

	Structure	$\log_{10}$ VI$_{exp}$	$\log_{10}$ VI$_{calc}$	Δ
1k	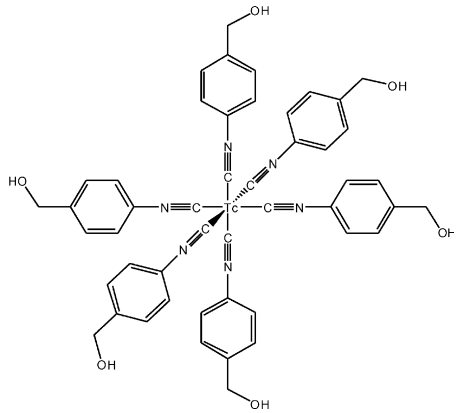	0.38	0.38	0.00
1l	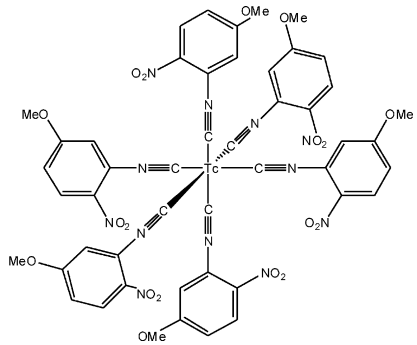	−0.02	−0.04	−0.02
1m	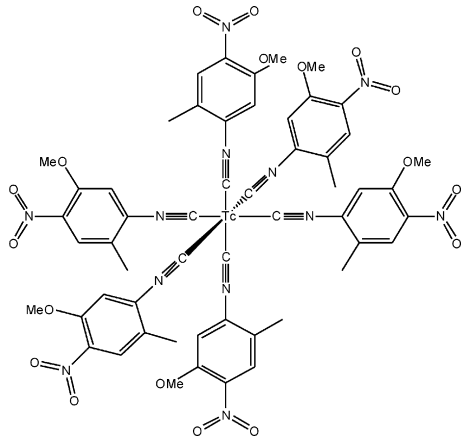	−0.06	−0.12	−0.06
2b	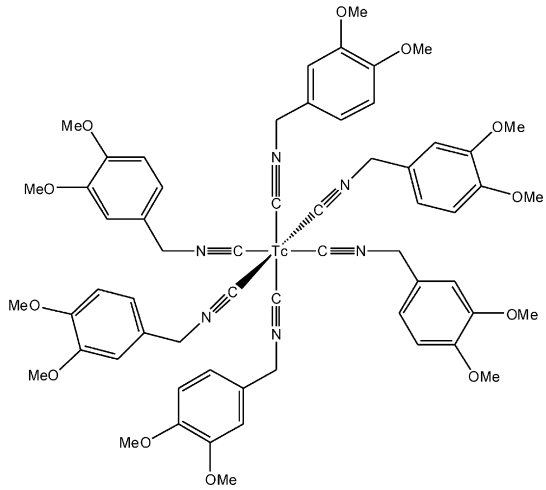	0.18	0.31	0.13

Table 5 (*Continued*)

	Structure	$\log_{10}$ VI$_{exp}$	$\log_{10}$ VI$_{calc}$	Δ
2c	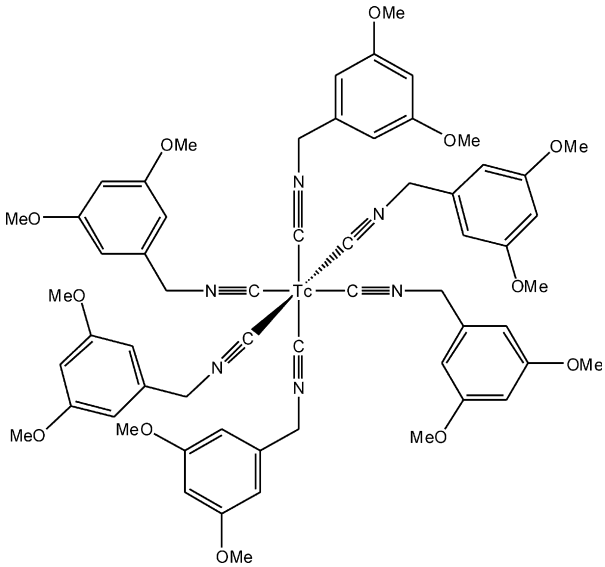	0.34	0.28	−0.06
2e	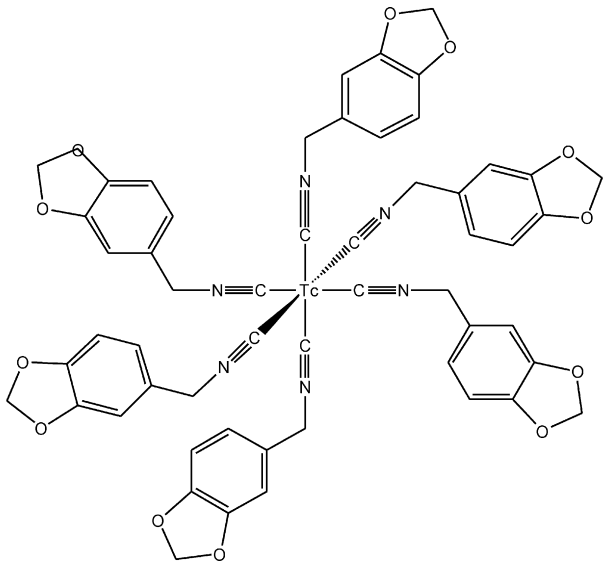	0.05	0.14	0.09
3a	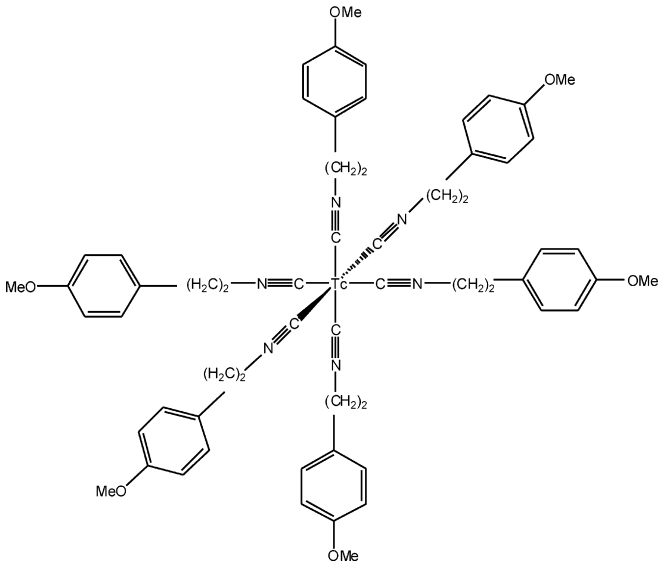	0.49	0.34	−0.15

Table 5 (*Continued*)

	Structure	$\log_{10}$ VI$_{exp}$	$\log_{10}$ VI$_{calc}$	Δ
3c	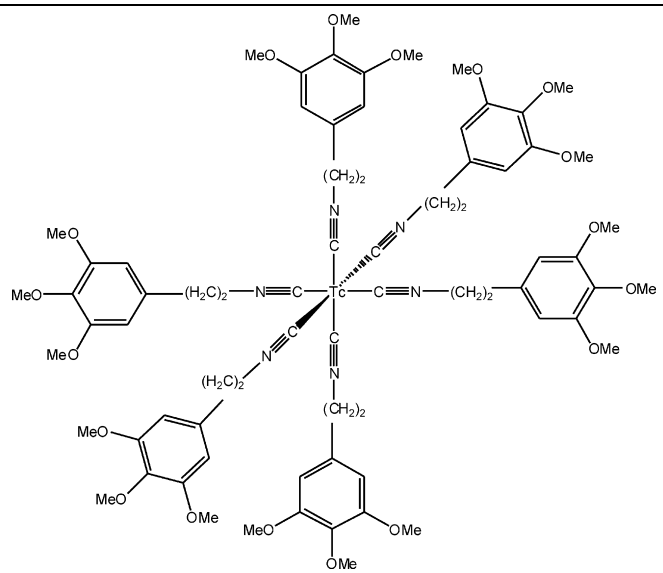	0.03	0.15	0.12

$\log_{10}$ VI$_{exp}$ refers to the $\log_{10}$ of the experimental verapamil index, the verapamil index represents the ratio of net uptake in the presence of verapamil over control, $\log_{10}$ VI$_{calc}$ to the QSAR calculated $\log_{10}$ of the verapamil index and Δ refers to the difference between the predicted and measured values.

'+' label and between −0.05 and 0.00 for the '−' label. The extension FPPOS refers to the fractional positive polar van der Waals surface area. The other two descriptors used are simple atom counts, a_count refers to a total atom count while a_nC refers to a count of the total number of carbon atoms in each technetium complex. The importance of the descriptor a_nC arising from the chemical composition of the dataset, i.e. predominately $(CH_2)_{n=0–2}$ areneisonitrile Tc(I) complexes.

Similarly, Table 7 (training set) and Table 8 (test set) present the results from the biodistribution QSAR analysis of the same 21 hexakis(areneisonitrile)technetium(I) complexes and ^{99m}Tc-sestamibi from Herman et al. [32]. Here, it was consistently feasible to construct QSAR models exhibiting cross-validated correlations of well above the benchmark 0.50 utilizing a total of just six molecular descriptors for the training set of 16 complexes. Our QSAR models perform very well when exposed to the blind test set of six compounds. Indeed, we are able to achieve q^2's above the benchmark 0.50 for both the renal QSAR and the hepatic QSAR. The poorest performance comes from the prediction of the renal uptake data for the test set exhibiting a $q^2 = 0.56$ which is still sufficiently predictive. The corresponding QSAR equations are given below:

Hepatic QSAR equation:

$$\begin{aligned}\log_{10}(\text{Blood/Liver})@30\,\text{min} &= 4.037 - (0.602 \times \text{PEOE_PC}-) \\ &\quad - (0.009 \times \text{PEOE_VSA} + 3) - (0.003 \times \text{PEOE_VSA-1}) \\ &\quad + (0.001 \times \text{SMR_VSA0}) - (0.345 \times \text{VDistEq}) \\ &\quad - (0.051 \times \text{bpol}) \qquad (2)\end{aligned}$$

Renal QSAR equation:

$$\begin{aligned}\log_{10}(\text{Blood/Kidney})@30\,\text{min} &= -16.267 - (53.418 \times \text{PC}-) - (53.339 \times \text{PEOE_PC}-) \\ &\quad + (2.680 \times \text{VDistEq}) + (0.301 \times \text{chi1}) \\ &\quad - (0.041 \times \text{dipoleX}) - (0.001 \times \text{weinerPath}) \qquad (3)\end{aligned}$$

The hepatic QSAR is dominated by PEOE descriptors based on the partial charge analysis of Gasteiger and Marsili described previously suggesting again that the distribution of molecular charge is important [34]. PEOE_PC− refers specifically to the total negative partial charge. The remaining three descriptors consist of SMR_VSA0, VDistEq and bpol. SMR refers to the molecular refractivity including implicit hydrogens and was derived by Wildman and Crippen [37], while the VSA0 label refers to the summation of the van der Waals surface where the refractivity is between 0.00 and 0.11. VDistEq is a summation of the entries in a matrix which describes specific internal distance metrics. The remaining descriptor used in the hepatic QSAR is bpol which refers to the sum of the absolute value of the difference between atomic polarizabilities of all bonded atoms in the molecule, the polarizabilities being taken from the *Handbook of Chemistry and Physics*. In conclusion, our correlation to the experimental $\log_{10}$(Blood/Liver) is based on a relationship of the total negative partial charge, the van der Waals surface area at specific points where the partial charge distribution satisfies a specific value range, together with an internal description of distance metrics and a summation of polarizabilities. In essence, it is dominated by aspects of the partial charge distribution which should come as a surprise since it is well known that properties such as formal charge play an important role in drug metabolism.

Table 6
Comparison of calculated and experimental verapamil index ($\log_{10}$ VI) of Tc(I)-isonitrile complexes in QSAR test set

	Structure	$\log_{10}$ VI_{exp}	$\log_{10}$ VI_{calc}	Δ
1b	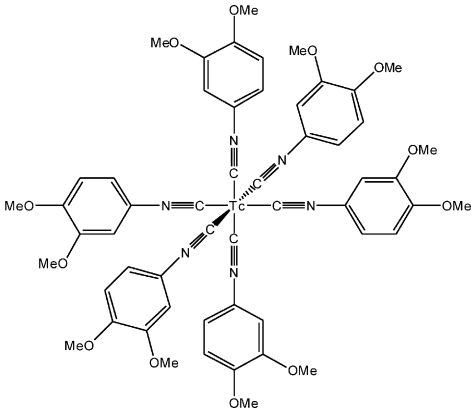	0.55	0.35	−0.20
1e	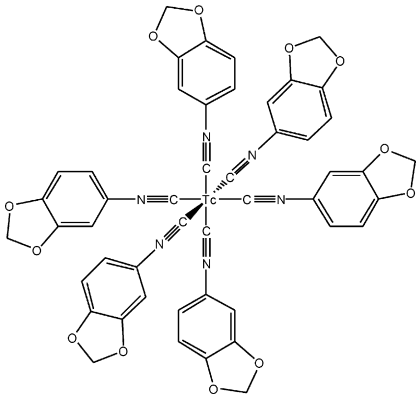	0.27	0.18	−0.09
1h	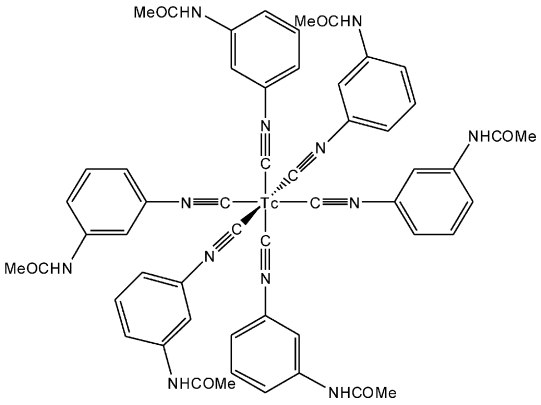	−0.11	0.63	0.74
2a	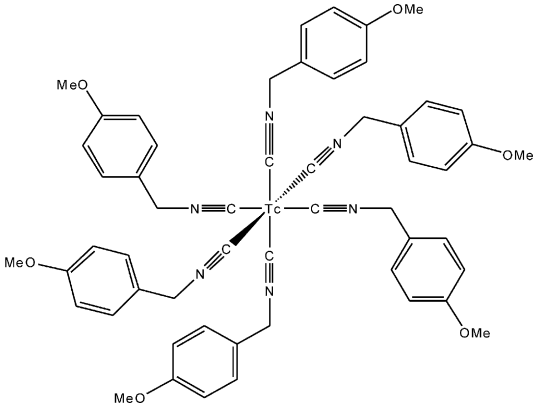	0.42	0.41	−0.01

Table 6 (*Continued*)

	Structure	$\log_{10}$ VI$_{exp}$	$\log_{10}$ VI$_{calc}$	Δ
2d	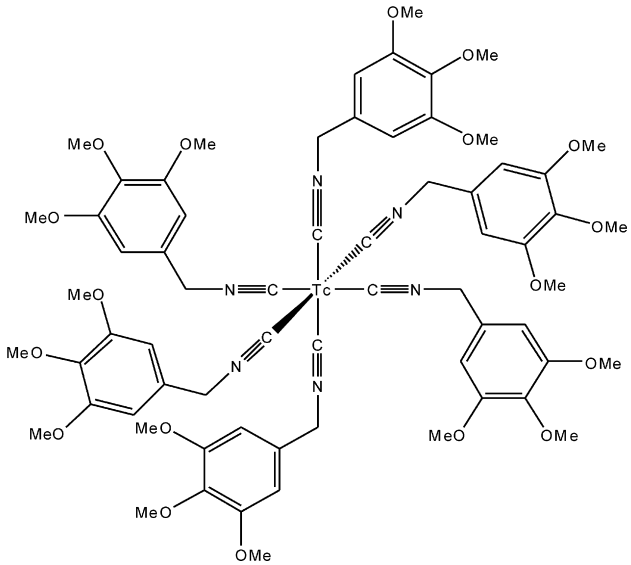	−0.10	0.22	0.32
3b	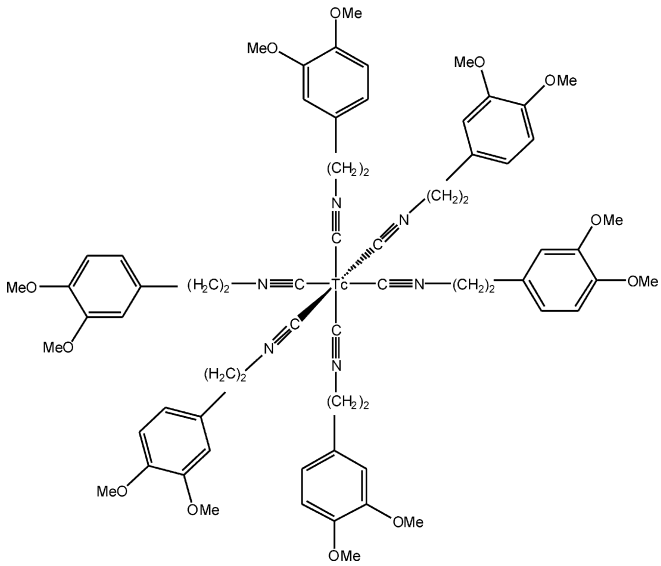	0.52	0.24	−0.28

$\log_{10}$ VI$_{exp}$ refers to the $\log_{10}$ of the experimental verapamil index, the verapamil index represents the ratio of net uptake in the presence of verapamil over control, $\log_{10}$ VI$_{calc}$ to the QSAR calculated $\log_{10}$ of the verapamil index and Δ refers to the difference between the predicted and measured values.

Table 7
Results from QSAR models of the biodistribution of the Tc(I)-isonitrile complexes in the training set

QSAR model	r^2	q^2	RMSE	RMSE$_{cv}$	n_{mols}	F
Hepatic						
$\log_{10}$(Blood/Liver) @30 min	0.97	0.96	0.11	0.25	16	56
Renal						
$\log_{10}$(Blood/Kidney) @30 min	0.85	0.82	0.26	0.28	16	8

$\log_{10}$(Blood/Liver) refers to the $\log_{10}${(%ID/g blood)/(%ID/g liver)}, $\log_{10}$(-Blood/Kidney) to the $\log_{10}${(%ID/g blood)/(%ID/g kidney)}, r^2 to the non-validated correlation, q^2 to the cross-validated correlation, F to the measure of the statistical significance of the model, RMSE to the root mean square error and RMSE$_{cv}$ refers to the cross-validated root mean square error.

Table 8
Results from QSAR models of the biodistribution of the Tc(I)-isonitrile complexes in the test set

QSAR model	r^2	q^2	RMSE	RMSE$_{cv}$	n_{mols}
Hepatic					
$\log_{10}$(Blood/Liver) @30 min	0.01	0.78	0.11	0.44	6
Renal					
$\log_{10}$(Blood/Kidney) @30 min	0.85	0.56	0.25	0.43	6

$\log_{10}$(Blood/Liver) refers to the $\log_{10}${(%ID/g blood)/(%ID/g liver)}, $\log_{10}$(-Blood/Kidney) to the $\log_{10}${(%ID/g blood)/(%ID/g kidney)}, r^2 to the non-validated correlation, q^2 to the cross-validated correlation, RMSE to the root mean square error and RMSE$_{cv}$ refers to the cross-validated root mean square error.

The renal QSAR relationship is more balanced correlating both partial charge based descriptors and descriptors based more on describing molecular size and connectivity. These size based descriptors being the already described VDistEq, chi1 and a descriptor called the weinerPath. The chi1 descriptor refers to the atomic connectivity index (order 1) from Hall and Kier [38], while weinerPath is a summation of the entries in a matrix which describes specific internal distance metrics [39]. Total negative charge is again important to predicting uptake metabolism in the kidney (PC− and PEOE_PC−) while the *x*-coordinate component of the dipole moment dipoleX, derived from the partial charge description, is also found to be predictive.

4. Conclusions

This work illustrates the effectiveness of the application of a genetic algorithm to the method of developing technetium metal ligand parameters for Allinger's MM3 force field. The development of new metal ligand parameters to model the biological properties of organometallic complexes containing this important radionuclide provides an important tool for the researcher in the fields of bioinorganic chemistry and nuclear medicine. As we develop a library of such radionuclide ligand parameters for these important radiopharmaceuticals, we hope to provide the researcher with new tools in the battle to develop novel radiopharmaceuticals with enhanced therapeutic and imaging characteristics. In this work we have illustrated how these new parameters might be utilized in the development of quantitative structure–activity relationships to predict firstly the MDR Pgp cell uptake of a series of common chelating agents of technetium(I) radionuclides and secondly their biodistribution.

In the case of the $\log_{10}$ VI QSAR model, we were able to predict with excellent accuracy the competitive MDR Pgp cell uptake of a series of hexakis(areneisonitrile)technetium(I) complexes and ^{99m}Tc-sestamibi. In addition, our biodistribution QSAR models were able to predict with excellent accuracy the accumulation of the same technetium(I) complexes in both the liver and kidneys. As we develop our library of radionuclide ligand force field parameters, we will continue to provide a more rigorous analysis of the application of the QSAR methodology to the prediction of the biological properties of radiopharmaceuticals with larger and more diverse datasets.

Acknowledgment

This work was supported by the National Institute of Biomedical Imaging and Bioengineering grant EB00340.

Appendix A. Supplementary material

A complete set of the MM3 parameters described in this work is available as well as a table comparing modeled geometries to experimental for selected high and low rmsd complexes.

Supplementary data associated with this article can be found, in the online version, at doi:10.1016/j.jmgm.2006.04.007.

References

[1] S.S. Jurisson, J.D. Lydon, Potential technetium small molecule radiopharmaceuticals, Chem. Rev. 99 (1999) 2205–2218.
[2] S. Liu, D.S. Edwards, 99mTc-labeled small peptides as diagnostic radiopharmaceuticals, Chem. Rev. 99 (1999) 2235–2268.
[3] D.E. Reichert, J.S. Lewis, C.J. Anderson, Metal complexes as diagnostic tools, Coord. Chem. Rev. 184 (1999) 3–66.
[4] E. Prats, F. Aisa, M.D. Abos, L. Villavieja, F. Garcia-Lopez, et al., Mammography and 99mTc-MIBI scintimammography in suspected breast cancer, J. Nucl. Med. 40 (1999) 296–301.
[5] D. Piwnica-Worms, M.L. Chiu, M. Budding, J.F. Kronauge, R.A. Kramer, et al., Functional imaging of multidrug-resistant P-glycoprotein with an organotechnetium complex, Can. Res. 53 (1993) 977–984.
[6] V.V. Rao, M.L. Chiu, J.F. Kronauge, D. Piwnica-Worms, Expression of recombinant human multidrug resistance P-glycoprotein in insect cells confers decreased accumulation of technetium-99m-sestamibi, J. Nucl. Med. 35 (1994) 510–515.
[7] H.F. Kung, H.J. Kim, M.P. Kung, S.K. Meegalla, K. Plossl, et al., Imaging of dopamine transporters in humans with technetium-99m TRODAT-1, Eur. J. Nucl. Med 23 (1996) 1527–1530.
[8] M. Das, K. Mukhopadhyay, Dopamine transporter: functional implication in neurobehavioral disorders, J. Cell Tissue Res. 5 (2005) 487–496.
[9] H. Han, C.-G. Cho, P.T. Lansbury Jr., Technetium complexes for the quantitation of brain amyloid, Chem. Rev. 118 (1996) 4506–4507.
[10] J.A. Katzenellenbogen, M.J. Welch, F. Dehdashti, The development of estrogen and progestin radiopharmaceuticals for imaging breast cancer, Anticancer Res. 17 (1997) 1573–1576.
[11] F. Wüst, Use of [99mTc]technetium-labeled steroids as probes for steroid hormone receptors, Methods Mol. Biol. 176 (2001) 133–143.
[12] J.P. DiZio, C.J. Anderson, A. Davison, G.J. Ehrhardt, K.E. Carlson, et al., Technetium- and rhenium-labeled progestins: synthesis, receptor binding and in vivo distribution of an 11 beta-substituted progestin labeled with technetium-99 and rhenium-186, J. Nucl. Med. 33 (1992) 558–569.
[13] R.K. Hom, J.A. Katzenellenbogen, Technetium-99m-labeled receptor-specific small-molecule radiopharmaceuticals: recent developments and encouraging results, Nucl. Med. Biol. 24 (1997) 485–498.
[14] C. Hansch, P.P. Maloney, T. Fujita, R.M. Muir, Correlation of biological activity of phenoxyacetic acids with Hammett substituent constants and partition coefficients, Nature 194 (1962) 178–180.
[15] C. Hansch, A. Leo, Exploring QSAR Fundamentals and Applications in Chemistry and Biology, American Chemical Society, Washington, DC, 1995.
[16] A. Agarwal, P.P. Pearson, E.W. Taylor, H.B. Li, T. Dahlgren, et al., Three-dimensional quantitative structure–activity relationships of 5-HT receptor binding data for tetrahydropyridinylindole derivatives: a comparison of the Hansch and CoMFA methods, J. Med. Chem. 36 (1993) 4006–4014.
[17] C. Hansch, A. Leo, S.B. Mekapati, A. Kurup, QSAR and ADME, Bioorg. Med. Chem. 12 (2004) 3391–3400.
[18] C. Klein, D. Kaiser, S. Kopp, P. Chiba, G.F. Ecker, Similarity based SAR (SIBAR) as tool for early ADME profiling, J. Comput. Aided Mol. Des. 16 (2003) 785–793.
[19] R. Garg, A. Kurup, S.B. Mekapati, C. Hansch, Cyclooxygenase (COX) inhibitors: a comparative QSAR study, Chem. Rev. 103 (2003) 703–731.
[20] P. Wolohan, J. Yoo, M.J. Welch, D.E. Reichert, QSAR studies of copper azamacrocycles and thiosemicarbazones: MM3 parameter development and prediction of biological properties, J. Med. Chem. 48 (2005) 5561–5569.
[21] N.L. Allinger, Y.H. Yuh, J.H. Lii, Molecular mechanics. The MM3 force field for hydrocarbons, J. Am. Chem. Soc. 111 (1989) 8551–8566.
[22] K. Gundertofte, T. Liljefors, P.-O. Norrby, I. Pettersson, A comparison of conformational energies calculated by several molecular mechanics methods, J. Comput. Chem. 17 (1996) 429–449.

[23] P. Brandt, T. Norrby, B. Åkermark, P.-O. Norrby, Molecular mechanics (MM3*) parameters for ruthenium(II)–polypyridyl complexes, Inorg. Chem. 37 (1998) 4120–4127.
[24] T. Strassner, M. Busold, A. Herrmann Wolfgang, MM3 parametrization of four- and five-coordinated rhenium complexes by a genetic algorithm—which factors influence the optimization performance? J. Comput. Chem. 23 (2002) 282–290.
[25] P.-O. Norrby, P. Brandt, Deriving force field parameters for coordination complexes, Coord. Chem. Rev. 212 (2001) 79–109.
[26] T.R. Cundari, W. Fu, Genetic algorithm optimization of a molecular mechanics force field for technetium, Inorg. Chim. Acta 300–302 (2000) 113–124.
[27] J.W. Ponder, TINKER4.2, 2004.
[28] F.H. Allen, O. Kennard, 3D search and research using the Cambridge Structural Database, Chem. Des. Autom. News 8 (1993) 31–37.
[29] G. Schaftenaar, J.H. Noordik, MOLDEN: a pre- and post-processing program for molecular and electronic structures, J. Comput. Aided Mol. Des. 14 (2000) 123–134.
[30] C.I. Bayly, P. Cieplak, W.D. Cornell, P.A. Kollman, A well-behaved electrostatic potential based method using charge restraints for deriving atomic charges: the RESP model, J. Phys. Chem. 97 (1993) 10269–10280.
[31] Jaguar, 5.0 ed., Schrödinger, Inc., Portland, OR, 2004.
[32] L.W. Herman, V. Sharma, J.F. Kronauge, E. Barbarics, L.A. Herman, et al., Novel hexakis(areneisonitrile)technetium(I) complexes as radioligands targeted to the multidrug resistance P-glycoprotein, J. Med. Chem. 38 (1995) 2955–2963.
[33] Molecular Operating Environment, Chemical Computing Group Inc., Que., Canada, 1997–2004.
[34] J. Gasteiger, M. Marsili, Iterative partial equalization of orbital electronegativity—a rapid access to atomic charges, Tetrahedron 36 (1980) 3219–3288.
[35] J. Bernard, K. Ortner, B. Spingler, H.-J. Pietzsch, R. Alberto, Aqueous synthesis of derivatized cyclopentadienyl complexes of technetium and rhenium directed toward radiopharmaceutical application, Inorg. Chem. 42 (2003) 1014–1022.
[36] G. Bandoli, A. Dolmella, M. Porchia, F. Refosco, F. Tisato, Structural overview of technetium compounds, Coord. Chem. Rev. 214 (2001) 43–90.
[37] S.A. Wildman, G.M. Crippen, Prediction of physicochemical parameters by atomic contributions, J. Chem. Inf. Comput. Sci. 39 (1999) 868–873.
[38] L.H. Hall, L.B. Kier, Molecular connectivity chi indices for database analysis and structure-property modelling, in: Topological Indices and Related Descriptors in QSAR and QSPR; Gordon & Breach Science Publishers, Amsterdam, 1999, pp. 307–360.
[39] A.T. Balaban, Chemical graphs. XXXIV. Five new topological indexes for the branching of tree-like graphs, Theor. Chim. Acta 53 (1979) 355–375.